JOURNAL OF BONE AND MINERAL RESEARCH
Volume 24, Number 8, 2009
Published online on February 16, 2009; doi: 10.1359/JBMR.090226

Serum IGF-1 Determines Skeletal Strength by Regulating Subperiosteal Expansion and Trait Interactions

Shoshana Yakar,[1] Ernesto Canalis,[2] Hui Sun,[1] Wilson Mejia,[1] Yuki Kawashima,[1] Philip Nasser,[5] Hayden-William Courtland,[1] Valerie Williams,[5] Mary Bouxsein,[3] Clifford Rosen,[4] and Karl J. Jepsen[5]

ABSTRACT: Strong correlations between serum IGF-1 levels and fracture risk indicate that IGF-1 plays a critical role in regulating bone strength. However, the mechanism by which serum IGF-1 regulates bone structure and fracture resistance remains obscure and cannot be determined using conventional approaches. Previous analysis of adult liver-specific IGF-1–deficient (LID) mice, which exhibit 75% reductions in serum IGF-1 levels, showed reductions in periosteal circumference, femoral cross-sectional area, cortical thickness, and total volumetric BMD. Understanding the developmental sequences and the resultant anatomical changes that led to this adult phenotype is the key for understanding the complex relationship between serum IGF-1 levels and fracture risk. Here, we identified a unique developmental pattern of morphological and compositional traits that contribute to bone strength. We show that reduced bone strength associated with low levels of IGF-1 in serum (LID mice) result in impaired subperiosteal expansion combined with impaired endosteal apposition and lack of compensatory changes in mineralization throughout growth and aging. We show that serum IGF-1 affects cellular activity differently depending on the cortical surface. Last, we show that chronic reductions in serum IGF-1 indirectly affect bone strength through its effect on the marrow myeloid progenitor cell population. We conclude that serum IGF-1 not only regulates bone size, shape, and composition during ontogeny, but it plays a more fundamental role—that of regulating an individual's ability to adapt its bone structure to mechanical loads during growth and development.
J Bone Miner Res 2009;24:1481–1492. Published online on February 16, 2009; doi: 10.1359/JBMR.090226

Key words: IGF, acid labile subunit, binding proteins, osteoclast, osteoblast, bone fragility, bone strength, functional adaptation

Address correspondence to: *Shoshana Yakar, PhD, Department of Endocrinology/Diabetes and Bone Disease, The Mount Sinai School of Medicine, One Gustave L Levy Place, Box 1055, New York, NY 10029-6574, USA, E-mail: shoshana.yakar@mssm.edu*

INTRODUCTION

Decreased serum IGF-1 levels have been correlated with reduced bone mass[1] and increased fracture risk,[2] indicating that it plays a critical role in skeletal acquisition and strength. However, the biomechanical mechanisms by which IGF-1 regulates bone function and structure remain unclear.[3] Recent studies show that fracture risk is associated with alterations in bone diameter accompanied with changes in cortical thickness and trabecular bone mass.[4–7] Therefore, to study the complex effects of IGF-1 on skeletal strength, we need to consider cellular and molecular mechanisms in the context of biomechanics and to use an integrative rather than a conventional reductionist approach. This level of analysis does not rely on individual cellular or molecular mechanisms per se, but rather merges cellular activities on multiple bone surfaces with biomechanical changes to show their collective effects on bone strength.

Mouse models have provided remarkable insight into the relationship between IGF-1 and bone. Naturally occurring polymorphisms that affect *igf*-1 gene expression show complex changes in mouse skeletal structure.[8,9] Prior studies showed that serum IGF-1 levels did not correlate well with external bone size, a critical determinant of bone strength; C57BL/6J mice, with low serum IGF-1, have a larger bone diameter compared with C3H/HeJ mice, with increased circulating IGF-1.[10] Congenic mouse strains, however, show the opposite response, with increased IGF-1 exhibiting larger bone diameter.[11–15] Collectively, the one common structural alteration that correlates with serum IGF-1 is cortical bone area (Ct.Ar.), a measure of diaphyseal bone mass, in both mice and humans (independent of bone length).[15,16] Together, these studies suggest that circulating IGF-1 regulates bone mass relative to body weight and therefore may mediate the response of bone to mechanical loading.[17]

The authors state that they have no conflicts of interest.

[1]Division of Endocrinology, Diabetes and Bone Disease, Mount Sinai School of Medicine, New York, New York, USA; [2]Department of Research, Saint Francis Hospital & Medical Center, Hartford, Connecticut, USA; [3]Orthopedic Biomechanics Laboratory, Beth Israel Deaconess Medical Center, Harvard Medical School, Boston, Massachusetts, USA; [4]Maine Medical Center Research Institute, Scarborough, Maine, USA; [5]Leni & Peter W. May Department of Orthopaedics, Mount Sinai School of Medicine, New York, New York, USA.

IGF-1 effects on cellular activity have been studied in vivo and in vitro. IGF-1 increases osteoblast[18] and osteoclast[19] cell proliferation and differentiation and seems to be a coupling agent for bone formation and resorption through the regulation of the RANKL and its decoy receptor osteoprotegerin (OPG) (RANKL/OPG) axis.[20,21] Thus, it is conceivable that IGF-1 regulates the amount of bone (Ct.Ar.) by coordinating periosteal and endosteal surface expansions during growth through its effects on osteoblastic and osteoclastic cell populations. Nonetheless, relating osteoblast/osteoclast cell activities to bone strength requires understanding the biomechanical mechanisms by which cells alter bone structure and bone quality.

Studies using mouse models of IGF-1 or the IGF-1 receptor gene knockouts[22–26] provide significant insights into IGF-1 action on bone. Nevertheless, interpretation of the data are difficult because IGF-1 and IGF-1R-null mice exhibit increased lethality. Furthermore, severe organ defects in those mice make it hard to distinguish direct and indirect actions of IGF-1 on bone. Importantly, IGF-1 acts in a dual mechanistic mode as an endocrine or autocrine/paracrine hormone. Therefore, when studying the relationship between serum IGF-1 and bone strength, it is crucial to choose a model that allows differentiation between the relative contributions of endocrine and autocrine/paracrine IGF-1.

Liver-specific *igf1* gene-deficient (LID) mice exhibit 75% reductions in serum IGF-1 levels with no changes in skeletal *igf1* expression.[27] Analyses of the adult LID bones by pQCT and μCT showed reductions in periosteal circumference, femoral cross-sectional area, cortical thickness, and total volumetric BMD.[28,29] Hence, the LID mouse model established an essential role for serum (endocrine) IGF-1 in skeletal acquisition. However, the developmental sequences and the resultant anatomical changes that led to this adult phenotype are not clear. To understand how low levels of serum IGF-1 led to this adult phenotype, we assessed the skeletal morphology of LID mice from 4 to 52 wk of age. In contrast to previous studies, which compared specific bone traits at certain time points, we assessed the relationship among traits over time using a systems analysis. Similar analyses, done recently on inbred mouse strains, provide expectations of how changes in one trait are compensated by coordinated changes in other traits.[30] Because IGF-1 has multiple effects on different cellular populations in bone, we expected co-variation of traits in response to decreased serum IGF-1 levels. We found that reduced bone strength in LID mice resulted from impaired subperiosteal expansion combined with impaired endosteal apposition and lack of compensatory changes in mineralization throughout growth and aging. Moreover, we show that serum IGF-1 affects cellular activity differently depending on the cortical surface.

MATERIALS AND METHODS

Animals

LID mice were generated as previously described.[27] Mice were backcrossed 13 generations to the FVB/N background. Male mice were housed four per cage in a clean mouse facility, fed a standard mouse chow (Purina Laboratory Chow 5001; Purina Mills) and water ad libitum, and kept on a 12-h light:dark cycle. Animal care and maintenance were provided through the Mount Sinai School of Medicine AAALAC Accredited Animal Facility. All procedures were approved by the Animal Care and Use Committee of the Mount Sinai School of Medicine.

Serum hormones

Mice were bled through the mandibular vein, and serum samples were collected between 7:00 and 9:00 a.m. on a fed state at the indicated ages. Serum IGF-1, growth hormone (GH), and insulin levels were determined using commercial radioimmunoassays as previously described.[28,29,31] Serum levels of mouse IGF binding protein (IGFBP)-2 and IGFBP-3 were determined by ELISA developed using recombinant mouse proteins from R&D and monoclonal antibodies as previously described.[32]

Body composition

Body composition (fat and lean mass) was assessed in live (nonanesthetized) animals using MRI (EchoMRI 3-in-1; Echo Medical Systems). This technique allows serial measurements with high levels of precision and without affecting the subjects tested. The measurement of each mouse lasts 90 s, and the precision of the measurement is between 0.1 and 0.3 SD.

μCT

An eXplore Locus SP PreClinical Specimen Micro-Computed Tomography system (GE Healthcare, London, Ontario, Canada) was used to assess trabecular bone volume fraction and microarchitecture in the excised distal femoral metaphysis and cortical bone geometry at the midfemoral diaphysis, as previously described.[30] Morphometric variables were computed from the binarized images using direct, 3D techniques that do not rely on any prior assumptions about the underlying structure.[33,34] Femora were reconstructed at an 8.7-μm voxel resolution. For trabecular bone regions, we assessed bone volume fraction (BV/TV, %), trabecular thickness (Tb.Th, μm), trabecular number (Tb.N, mm^{-1}), and trabecular separation (Tb.Sp, μm). For cortical bone at the femoral midshaft, we measured the average total cross-sectional area inside the periosteal envelope (TtAr, mm^2), the cortical bone and medullary area within this same envelope (CtAr, mm^2 and MaAr mm^2, respectively), the bone area fraction (CtAr/TtAr, %), and the average cortical thickness (CtTh, μm). All regions of analysis were standardized according to anatomical landmarks. Cortical and trabecular regions were individually thresholded using a standard thresholding algorithm[35] to segment bone and nonbone voxels. The μCT images were used to quantify tissue mineral density (TMDn), which is the average mineral value of the bone voxels only and is expressed in hydroxyapatite (HA) density equivalents. TMDn was calculated by converting the grayscale output of bone voxels in Hounsfield units (HUs) to mineral values (mg/ml of HA) through the use of

a calibration phantom containing air, water, and hydroxyapatite (SB3; Gamex RMI, Middleton, WI, USA). The same calibration phantom was included in all scans to adjust mineral density measurements for the variation in X-ray attenuation inherent to independent scan sessions. A validation study using 44 mouse femora showed that tissue mineral content correlated linearly ($p < 0.01$) with both ash weight/hydrated weight and ash weight/dry weight (data not shown).

Mechanical testing

Mouse femora from 20-wk-old control and LID mice were tested to failure by four-point bending using a servohydraulic materials testing system (Instron, Canton, MA, USA). This mechanical test allows comparison of the structural properties of stiffness, maximum load, postyield deflection, and work-to-failure. Femora were placed with the anterior surface down on two lower supports. The lower and two upper supports were set apart at 6.35 and 2.2 mm, respectively. Loading was centered over the midshaft. Displacement was applied at 0.05 mm/s until failure. All mechanical properties were calculated from the load and displacement curves, as described previously.[30]

Histomorphometry

Mice were injected with calcein (10 mg/kg) at days 7 and 2 before death (for the 4- and 8-wk-old groups) or at days 12 and 2 before death (for the 20-wk-old group). Femora were dissected, fixed in 10% neutral-buffered formalin, dehydrated, and embedded undecalcified in polymethyl methacrylate. Longitudinal sections of the distal femora, 5 μm thick, were cut on a Microm microtome (Microm; Richards-Allan Scientific, Kalamazoo, MI, USA) and stained with toluidine blue. Static parameters of bone formation and resorption were measured at a standardized site in the distal femoral metaphysis using OsteoMeasure (Osteometrics, Atlanta, GA, USA). Relative trabecular bone volume (BV/TV), osteoid surface (OS/BS, %), eroded surface (ES/BS, %), osteoblast or osteoclast number per bone perimeter (NOb/BPm, NOc/BPm), and osteoblast or osteoclast number per total area (NOb/Tar, NOc/Tar) were measured. For dynamic histomorphometry, mineralizing surface per bone surface (MS/BS, %) and mineral apposition rate (MAR, μm/d) were measured in unstained 10-μm sections under UV light, using a B-2A set long pass filter consisting of an excitation filter ranging from 450 to 490 nm (nm), a barrier filter at 515 nm, and a dichroic mirror at 500 nm. Bone formation rate per bone surface (BFR, $\mu m^3/\mu m^2/d$) was calculated. The terminology and units used are those recommended by the Histomorphometry Nomenclature Committee of the American Society for Bone and Mineral Research.[36]

Fluorescent-activated cell sorting

Flow cytometry was used to identify hematopoietic cells of the lymphoid or myeloid lineages that contribute to skeletal development. Bone marrow cells were harvested from the femur. The cells were washed with PBS and resuspended in staining buffer (PBS, 0.5% FBS, 0.09% sodium azide). Cells (10^6) were preincubated with rat anti-mouse CD16/CD32 (1 μg; BD Biosciences) for 10 min at 4°C to block Fc receptors. Cells were incubated for 30 min at 4°C with Alexa Fluor 647-conjugated rat anti-mouse CD11b or B220 (BD Biosciences). The cells were washed with cold PBS buffer and resuspended in 100 μl of staining buffer. Cells were washed twice with cold staining buffer and resuspended in PBS containing 1% paraformaldehyde. Cell acquisition was performed in a flow cytometer (FACScan; Becton Dickinson), and a minimum of 10,000 events was acquired for each test. Data were analyzed with FlowJow software (version 7.2). R-Phycoerythrin (PE)-conjugated mouse IgG_{2b} and Alexa Fluor 647-conjugated mouse IgG_{2a}, isotype controls were used.

Statistical analysis

Mean values for body weight (BW), body composition, serum hormones, histomorphometrical parameters, and μCT measurements were calculated for each genotype, and significant differences were assessed using *t*-tests with a significance threshold of $p < 0.05$. To correlate whole morphological bone traits, Pearson correlations were calculated for trait comparisons using the raw data from individual genotypes. For each correlation analysis, the threshold of $p < 0.05$ significance was chosen (GraphPad Software, San Diego, CA, USA).

RESULTS

Young adult LID mice fail to maintain normal body weight and manifest insulin resistance

LID mice were generated using the Cre/loxP system as described previously.[27] We followed the male LID mice on an inbred FVB/N strain from 4 to 52 wk. Body weight of LID mice did not differ significantly from controls up to 8 wk of age. However, starting at ~8 wk, the age-related gain of body weight slowed appreciably for LID mice, resulting in significant reductions in body weight relative to controls after 12 wk of age (Fig. 1A). To study whether the differences in body weight resulted from alterations in body composition, we evaluated lean and fat mass using MRI throughout growth (Fig. 1B). Lean and fat mass did not differ significantly between control and LID mice. LID mice exhibited 75% reductions in serum IGF-1 throughout growth and adulthood (Fig. 1C) and secondary increases in serum GH levels (Fig. 1D), which normalized at 32 wk. In our previous study, we showed that increased GH levels in the LID mice antagonized insulin action in muscle, liver, and fat and therefore led to insulin resistance. As seen in Fig. 1E, LID mice had increased serum insulin levels starting at 4 wk (when GH started to elevate under normal physiological conditions); at 52 wk, insulin levels of LID mice did not differ from those of control mice, most likely because of natural age-related increases in serum insulin in controls. Despite the hyperinsulinemia and insulin resistance throughout growth, LID mice remained normoglycemic (Fig. 1F). In the circulation, the main carrier of IGF-1 is IGFBP-3. In control mice, serum IGFBP-3

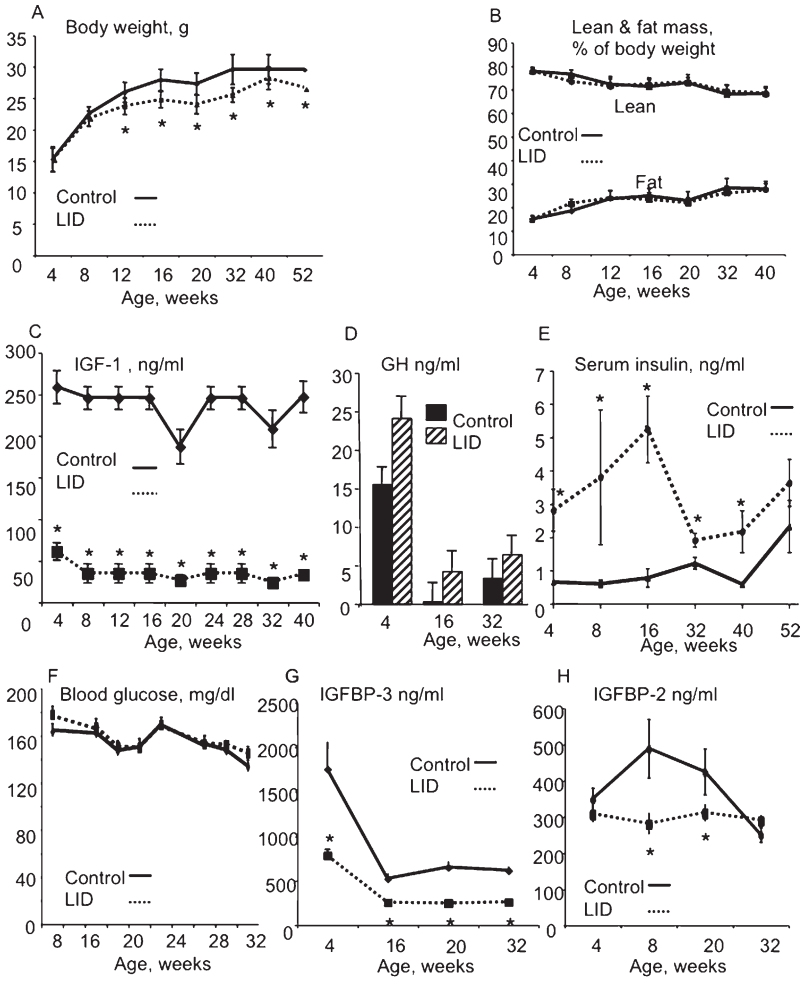

FIG. 1. Control and LID mice were followed from 4 to 52 wk of age. Body weight (A) and body composition (B) were followed monthly by MRI. Serum was obtained through the mandibular vein once a month, and IGF-1 (C), GH (D), insulin (E), blood glucose (F), IGFBP-3 (G), and IGFBP-2 (H) levels were analyzed. Results are presented as mean ± SE of at least 40 mice per age group per genotype.

peaked at 4 wk of age (together with GH and serum IGF-1) and decreased with age (~25% of levels seen at 4 wk). LID mice showed significant reductions (~50% compared with controls) in serum IGFBP-3 levels starting at 4 wk of age (Fig. 1G), despite increases in GH levels, possibly caused by protein degradation, because liver IGFBP-3 expression levels in LID mice are similar to controls (data not shown). LID mice showed significant reductions in serum IGFBP-2 levels starting at 8 wk of age (Fig. 1H), likely because of increased serum insulin[37] or GH levels[38] and may directly or indirectly be involved in the skeletal phenotype of the LID mice.

Serum IGF-1 does not affect cancellous bone

To relate changes in serum IGF-1 to bone accrual and skeletal integrity, we assessed trabecular bone at the distal femur. We observed an age-related decrease in bone volume/total volume (BV/TV) in both LID and WT mice. μCT analysis showed no significant differences in bone volume fraction (BV/TV; Fig. 2A) and no differences in trabecular tissue mineral density (TMD, mg/HA; Fig. 2B) between control and LID mice throughout development and adulthood. Similarly, no significant differences in trabecular thickness (Tb.Th.) or trabecular spacing (Tb.Sp.) were found between LID and controls, although LID mice showed a tendency for decreased Tb.Th. and increased Tb.Sp. (Table 1). These data were confirmed by histomorphometry (Fig. 2). At 20 wk, LID mice showed minor increases in percent eroded surface/bone surface (%Es/Bs), percent osteoclast surface/bone surface (%OCs/Bs), and number of osteoclast per total bone area (N.OC/Ta 1/mm^2; Fig. 2C–2E). This was accompanied by increases in percent osteoid surface (%Os/Bs; Fig. 2F), with no changes in percent mineralized surface (%Ms/Bs; data not shown). Mineral apposition rate (MAR) did not differ significantly between LID and control mice at 8 or 20 wk of age (data not shown). BFR, on the other hand, increased significantly in LID mice at 20 wk (controls: 0.004 ± 0.00 $\mu m^3/\mu m^2$/d versus LIDs: 0.005 ± 0.001 $\mu m^3/\mu m^2$/d). These data suggest that, in LID mice, compensatory increases in serum GH stimulate osteoblastic activity in the endosteal surface (evident by increases in osteoid surface). However, because no differences in MAR were evident, it may point to a lag in mineralization in the LID mice. Indeed, we found that mineralization lag time increased 3-fold in LID mice compared with controls (controls: 0.79 ± 0.15 d; LID: 3.02 ± 0.30 d). Although these results also suggested that skeletal IGF-1 expression increased, we were unable to detect differences in *igf-1 osteocalcin*, *OPG,* or *RANKL* gene expression in femoral diaphyses between control and LID

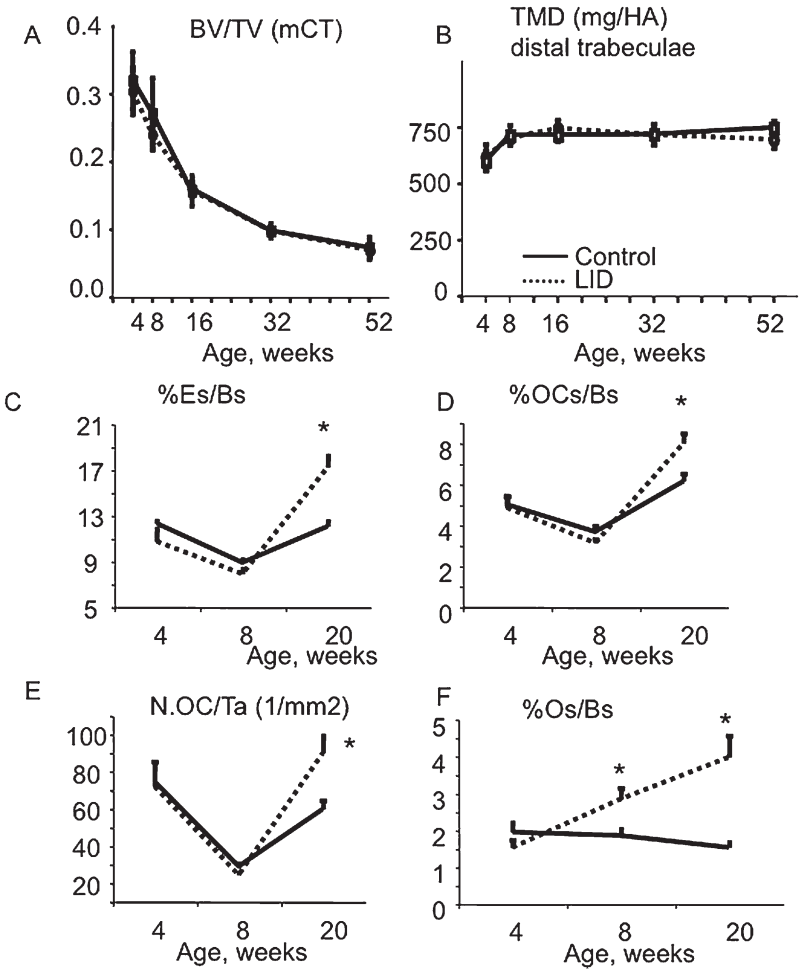

FIG. 2. Trabecular bone fraction does not differ significantly between control and LID mice. Trabecular bone parameters were assessed by μCT, and BV/TV (A) and TMD (B) were measured at the distal femur of formalin-fixed bones. Histomorphometry was performed on plastic bone sections from the distal femur; %Er.Bs (C), %OCs/Bs (D), N.OC/Ta (E), and %Os/Bs (F) were determined at 4, 8, and 20 wk of age. Results are presented as mean ± SE of $n = 6$ mice per age group per genotype.

mice (data not shown). Overall, the μCT and histomorphometric analyses showed no significant changes in trabecular bone acquisition or architecture between control and LID mice up to 8 wk of age and only minor changes in Tb.Th. after this age.

Serum reductions in IGF-1 impair subperiosteal expansion of the cortical envelope

Cortical bone architecture was evaluated at the femoral midshaft using μCT (Table 2). Our analysis showed no significant differences in cortical bone parameters between LID and control mice at 4 wk of age, suggesting that liver-derived IGF-1 (endocrine IGF-1) affects skeletal integrity starting at an early pubertal age (i.e., after 4 wk). These data suggested that the autocrine/paracrine action of IGF-1, which is normal in the skeleton of LID mice, is sufficient to establish bone size at 4 wk. Nonetheless, whereas in control mice there is a sharp increase in serum IGF-1 starting at 4 wk, which correlates with bone accrual, LID mice show 75% reductions in serum IGF-1 relative to controls and exhibit impaired age-related gains in total bone area and marrow area (Fig. 3). However, starting at 8 wk of age, LID mice exhibited significant reductions in total bone area (Tt.Ar; Fig. 3A), marrow area (Ma.Ar; Fig. 3B), and cortical area (Ct.Ar; Fig. 3C) relative to controls. Despite these reductions, femoral cortical tissue mineral density (TMD) did not differ between control and LID mice (Fig. 3D). The differences in morphology between LID and controls remained significant after the traits were corrected for body weight by linear regression analysis. Notably, after 16 wk, marrow area decreased with age for LID mice, indicating that the endosteal surface was undergoing apposition, which is opposite to the continued endosteal expansion expected during growth for male mice (and seen in controls). Polar moment of inertia (J), a calculated value indicative of bone stiffness and strength in bending (Fig. 3E), decreased in LID mice starting at 8 wk of age. Four-point bending tests at 20 wk of age showed 20% reductions in whole bone stiffness and maximum load (independent of body weight), but no changes in ductility in LID mice (Fig. 3F).

Interactions among morphological and compositional traits are impaired in LID mice

To understand whether the morphological differences between LID and control mice arose from differences in body weight (BW), we analyzed the relationship between morphological traits and BW. Bone slenderness (Tt.Ar/Le)

TABLE 1. μCT Analysis at the Distal Femur of Control and LID Mice at the Indicated Ages

		Distal femur (trabecular bone)	
		Control	*LID*
4 wk	BV/TV (%)	0.32 ± 0.02	0.30 ± 0.02
	Tb.Th (mm^2)	0.035 ± 0.001	0.036 ± 0.001
	Tb.Sp (mm)	0.14 ± 0.03	0.18 ± 0.03
	TMD (mg/ml)	614.7 ± 18.6	633.3 ± 28.1
8 wk	BV/TV (%)	0.27 ± 0.001	0.23 ± 0.001
	Tb.Th (mm^2)	0.035 ± 0.001	0.033 ± 0.001
	Tb.Sp (mm)	0.14 ± 0.001	0.15 ± 0.001
	TMD (mg/ml)	717.1 ± 22.0	696.9 ± 11.0
16 wk	BV/TV (%)	0.16 ± 0.001	0.16 ± 0.001
	Tb.Th (mm^2)	0.035 ± 0.001	0.032 ± 0.001
	Tb.Sp (mm)	0.22 ± 0.001	0.23 ± 0.001
	TMD (mg/ml)	718.7 ± 10.9	746.7 ± 14.4
32 wk	BV/TV (%)	0.1 ± 0.001	0.1 ± 0.001
	Tb.Th (mm^2)	0.04 ± 0.001	0.03 ± 0.001
	Tb.Sp (mm)	0.3 ± 0.00	0.4 ± 0.03
	TMD (mg/ml)	722.2 ± 16.8	719.1 ± 17.1
52 weeks	BV/TV (%)	0.07 ± 0.001	0.07 ± 0.001
	Tb.Th (mm^2)	0.04 ± 0.001	0.03 ± 0.001
	Tb.Sp (mm)	0.50 ± 0.02	0.50 ± 0.02
	TMD (mg/ml)	750.9 ± 11.5	697.5 ± 14.9

Results are presented as mean ± SD of $n > 8$ mice age per group per genotype.

TABLE 2. μCT Analysis at the Femoral Midshaft of Control and LID Mice at the Indicated Ages

		Femoral midshaft (cortical bone)	
		Control	*LID*
4 weeks	Total area (mm^2)	1.03 ± 0.08	0.96 ± 0.05
	Marrow area (mm^2)	0.57 ± 0.04	0.54 ± 0.03
	Cortical area (mm^2)	0.47 ± 0.04	0.42 ± 0.02
	CtTh (mm)	0.14 ± 0.01	0.13 ± 0.00
	TMD	1087.50 ± 16.59	1124.50 ± 27.16
	Jo	0.13 ± 0.02	0.11 ± 0.01
8 weeks	Total area (mm^2)	1.42 ± 0.05	1.19 ± 0.02*
	Marrow area (mm^2)	0.67 ± 0.03	0.61 ± 0.02*
	Cortical area (mm^2)	0.75 ± 0.02	0.59 ± 0.01*
	CtTh (mm)	0.19 ± 0.00	0.16 ± 0.00*
	TMD	1236.68 ± 10.31	1223.61 ± 14.74
	Jo	0.26 ± 0.02	0.17 ± 0.00*
16 weeks	Total area (mm^2)	1.52 ± 0.02	1.25 ± 0.02*
	Marrow area (mm^2)	0.78 ± 0.01	0.64 ± 0.01*
	Cortical area (mm^2)	0.73 ± 0.01	0.61 ± 0.01*
	CtTh (mm)	0.18 ± 0.00	0.16 ± 0.00*
	TMD	1295.66 ± 6.1	1302.05 ± 14.09
	Jo	0.28 ± 0.01	0.19 ± 0.01*
32 weeks	Total area (mm^2)	1.59 ± 0.02	1.19 ± 0.01*
	Marrow area (mm^2)	0.81 ± 0.02	0.58 ± 0.01*
	Cortical area (mm^2)	0.78 ± 0.01	0.61 ± 0.01*
	CtTh (mm)	0.19 ± 0.00	0.17 ± 0.00*
	TMD	1299.39 ± 9.62	1336 ± 16.99
	Jo	0.31 ± 0.01	0.18 ± 0.00*
52 weeks	Total area (mm^2)	1.64 ± 0.87	1.22 ± 0.02*
	Marrow area (mm^2)	0.87 ± 0.03	0.59 ± 0.01*
	Cortical area (mm^2)	0.77 ± 0.02	0.63 ± 0.00*
	CtTh (mm)	0.18 ± 0.00	0.17 ± 0.00
	TMD	1307.63 ± 8.69	1324.34 ± 4.20
	Jo	0.32 ± 0.02	0.19 ± 0.00*

Results are presented as mean ± SD of $n > 8$ mice age per group per genotype.

* $p < 0.05$.

was calculated as the ratio of total area, Tt.Ar, and bone length, Le, and is a measure of the amount of lateral growth (expansion) relative to longitudinal growth. LID mice had a slender bone phenotype (as represented by a small Tt.Ar/Le value) starting at puberty (4 wk) and continuing throughout development (Fig. 4A), indicating that reduced serum IGF-1 impaired the amount of subperiosteal expansion relative to longitudinal growth. In control mice, we observed a significant positive relationship between Tt.Ar/Le and BW, implying that the male femoral diaphysis adapted to increasing body weight through subperiosteal expansion (i.e., increased Tt.Ar relative to length; Fig. 4B). In contrast, LID mice showed no relationship between Tt.Ar/Le and body weight. This suggested that expansion of the subperiosteal surface during growth was impaired in LID mice and could not be used as a mechanism to adapt structurally to the age-related increase in body weight.

We postulated that male LID mice would compensate for their slender phenotype by increasing mineralization and/or by increasing bone mass through endosteal infilling. As seen in Fig. 4C, a measure of relative cortical area (RCA = Ct.Ar/Tt.Ar) was significantly increased for LID mice at 32 and 52 wk. Indeed, the relationship between RCA and body weight increased significantly in LID mice but not in controls (Fig. 4D). This indicated that the subperiosteal expansion required to match bone size with body weight was inhibited in LID mice but that LID femora attempted to attain a mechanically functional structure through changes in marrow expansion. This may explain the age-related decrease in Ma.Ar, observed for LID mice after 16 wk of age (Fig. 4B). These differences in subperiosteal and endosteal expansion resulted in LID femora having significantly reduced cortical area relative to body weight throughout all age groups ($p < 0.05$, ANCOVA; Fig. 4E). This indicated that, in addition to impairing periosteal expansion, the reduced serum IGF-1 also impaired the amount of marrow infilling leading to reduced bone mass.

We further tested whether LID mice also compensated for their slender phenotype by increasing the degree of tissue mineralization (TMD). When the effects of body weight were removed by partial regression analysis, we found significant negative correlations between slenderness and TMD in both LID and control mice ($R^2 = 0.13$, $p <$ 0.03–0.04), as expected. No differences in the slope and intercepts were observed between LID and controls ($p >$ 0.43, ANCOVA; data not shown). This indicated that, for both control and LID mice, femora that tended to be more slender (reduced Tt.Ar/Le) relative to body weight also tended to have higher TMD. The similarity in these regressions plus the fact that LID and control mice showed similar TMD values at each age suggested that LID mice did not manifest compensatory changes in mineralization beyond those observed for control mice.

Taken together, our data suggested that LID mice have impaired subperiosteal expansion, leading to slender bones. To adapt the structure so that bone stiffness matches weight-bearing loading demands, LID mice attempted to

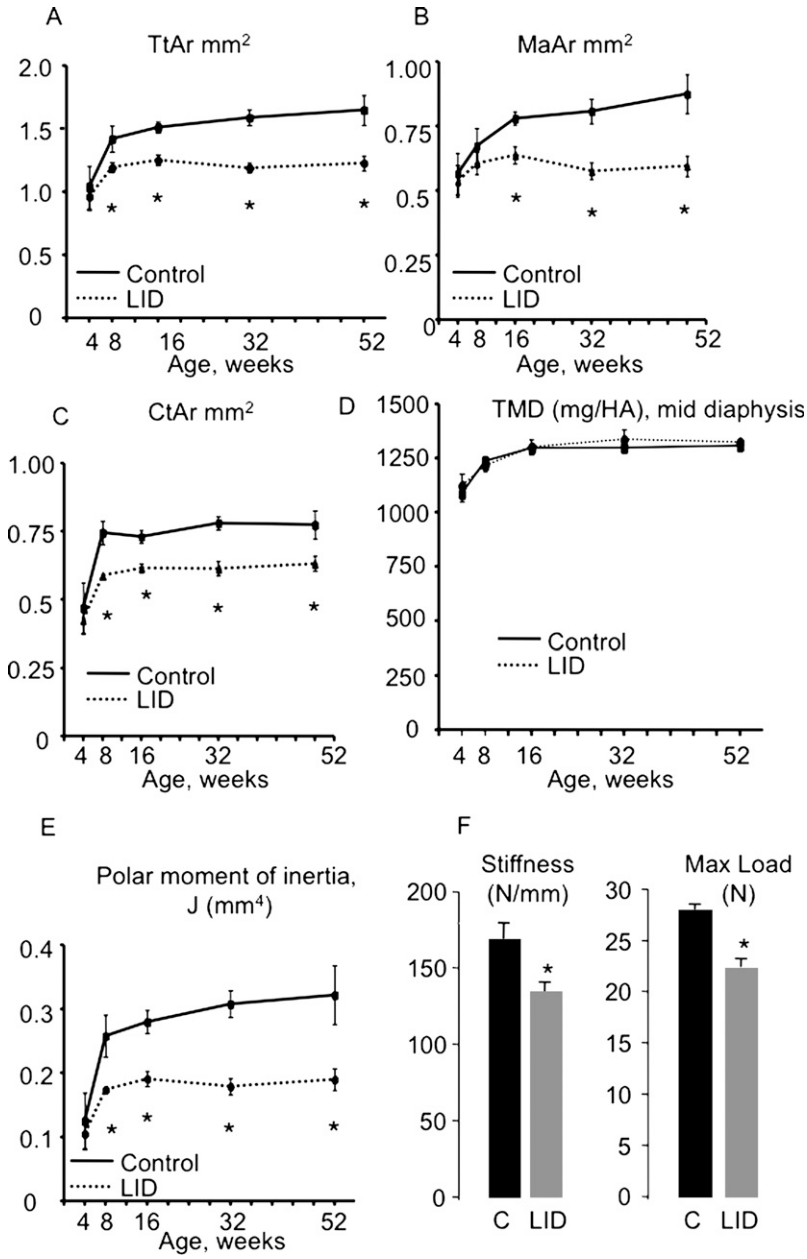

FIG. 3. LID mice have slender and more fragile bones. Cortical bone parameters were assessed during growth at the femoral midshaft using μCT. LID mice show reduced Tt.Ar. (A), Ma.Ar (B), and Ct.Ar (C) starting at 8 wk of age. TMD (D), measured by μCT, did not differ significantly between control and LID mice at all ages. LID mice cannot restore mechanical properties; LID mice show decreased polar moment of inertia (E) throughout growth and reduced stiffness and max load at four-point bending assay at 20 wk of age (F). Results are presented as mean ± SD of $n > 8$ mice per age group per genotype.

compensate for the slender phenotype by decreasing marrow area but did not compensate by increasing mineralization. Importantly, the reduced serum IGF-1 limited the amount of marrow infilling and thus impaired the process of functional adaptation, resulting in significantly reduced whole bone stiffness and strength (Fig. 3F).

LID mice exhibit decreased marrow osteoclasts progenitors

To understand the cellular mechanism that leads to impaired periosteal expansion in LID mice, we studied marrow stromal cell (MSC) differentiation into osteoblast-like cells, as well as the potential of nonadherent cells to differentiate into osteoclasts. MSC cultures derived from control and LID mice at different ages (4, 8, 16, 32, and 52 wk of age) showed no significant differences in the number of alkaline phosphatase–positive colonies (data not shown). These results suggested that LID and control mice have a similar potential to develop osteoblast-like colonies in vitro. Nonadherent cells derived from LID and control mice (at the indicated ages) were stimulated with macrophage-colony stimulating factor (M-CSF) and RANKL to drive osteoclastogenesis (Fig. 5A). The number of $TRACP^+$ (multinucleated) cells in cultures derived from LID mice was lower compared with controls, albeit not significantly at any of the ages. These in vitro data suggest that the number of osteoclast precursors in the

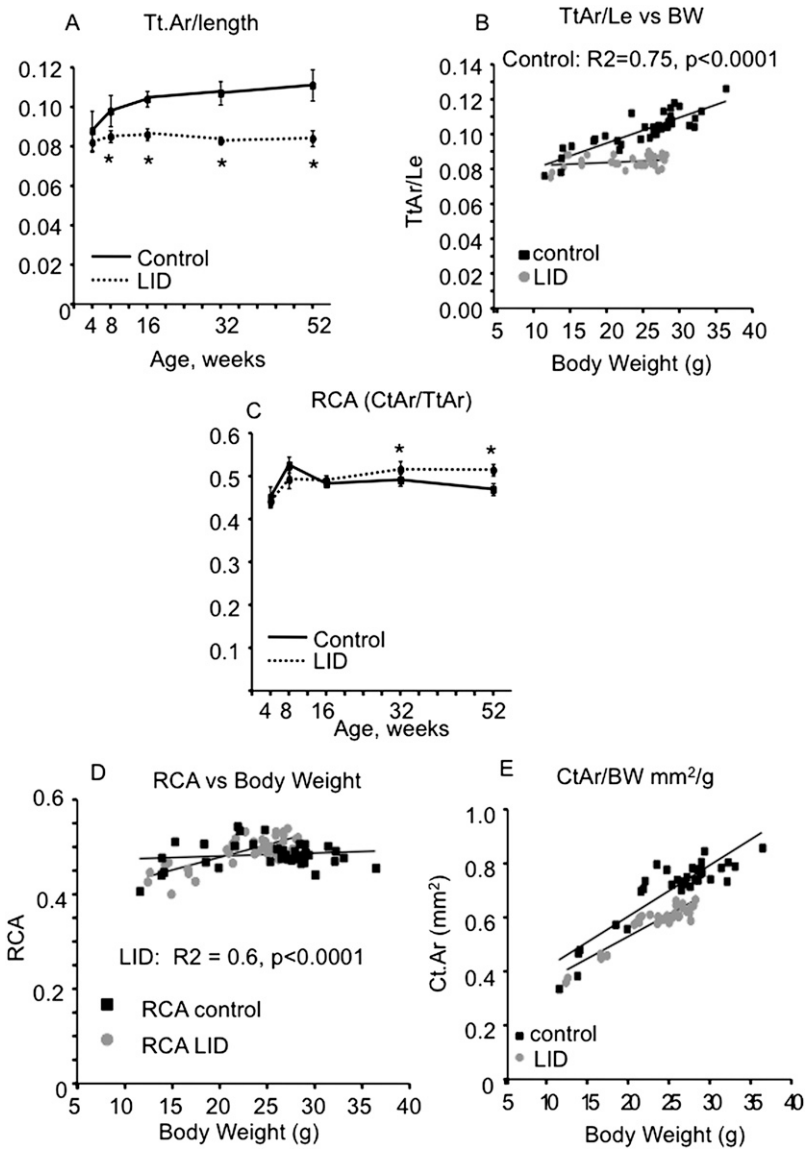

FIG. 4. LID mice exhibit impaired co-variation of morphological traits (obtained by μCT). LID mice have slender bones throughout growth starting at 4 wk (Tt.Ar/length) (A). Control mice show a positive relationship between Tt.Ar/length and body weight, whereas LID mice do not (B). LID mice exhibit an increase in relative cortical area, RCA, at 32 and 52 wk of age (C). LID mice show a positive relationship between RCA and body weight (D), suggesting that these mice compensate for the slender bones by increasing cortical area. Both control and LID mice show positive relationship between Ct.Ar and body weight (E). Results are presented as mean ± SD of $n > 8$ mice age per group per genotype.

nonadherent population derived from LID mice might be decreased. To address this possibility, we used ex vivo flow cytometry analysis of bone marrow–derived cells from control and LID mice during growth. Osteoclast precursors, which originate from the monocyte/macrophage cell lineage, express the CD11b/Mac-1 surface antigen, which mediates cell adhesion. LID mice showed a significant and consistent decrease in $CD11b^+$ cells in marrow (Fig. 5B), suggesting a decrease in the number of myeloid progenitor cell population. The lymphoid cell lineage was followed throughout development using the B220/CD19 surface antigen (Fig. 5C). A significant reduction in the lymphoid lineage was noticed at 4 wk of age (approximately when external bone size is determined) and did not differ from controls thereafter. A subgroup of the lymphoid cells express membrane bound and secreted RANKL, which is critical for osteoclastogenesis. Taken together, these in vitro/ex vivo data suggest that serum IGF-1 deficiency, as seen in LID mice, leads to reduction in marrow osteoclast progenitors and subsequently to impaired osteoclastogenesis on the endosteal surface. The reduced endosteal resorption may be a factor leading to the inhibition of subperiosteal expansion.

DISCUSSION

Our study combined phenotypic and functional analyses of mouse femora, allowing a more comprehensive understanding of how alterations in serum IGF-1 affect bone strength. We studied the LID mouse model (on a pure FVB/N genetic background) during growth and development and assessed the relationships among serum IGF-1 levels, bone mass, architecture, and bone strength. Reduced serum levels of IGF-1 in LID mice were associated with the development of slender bones during growth. This slender phenotype was not simply related to serum IGF-1

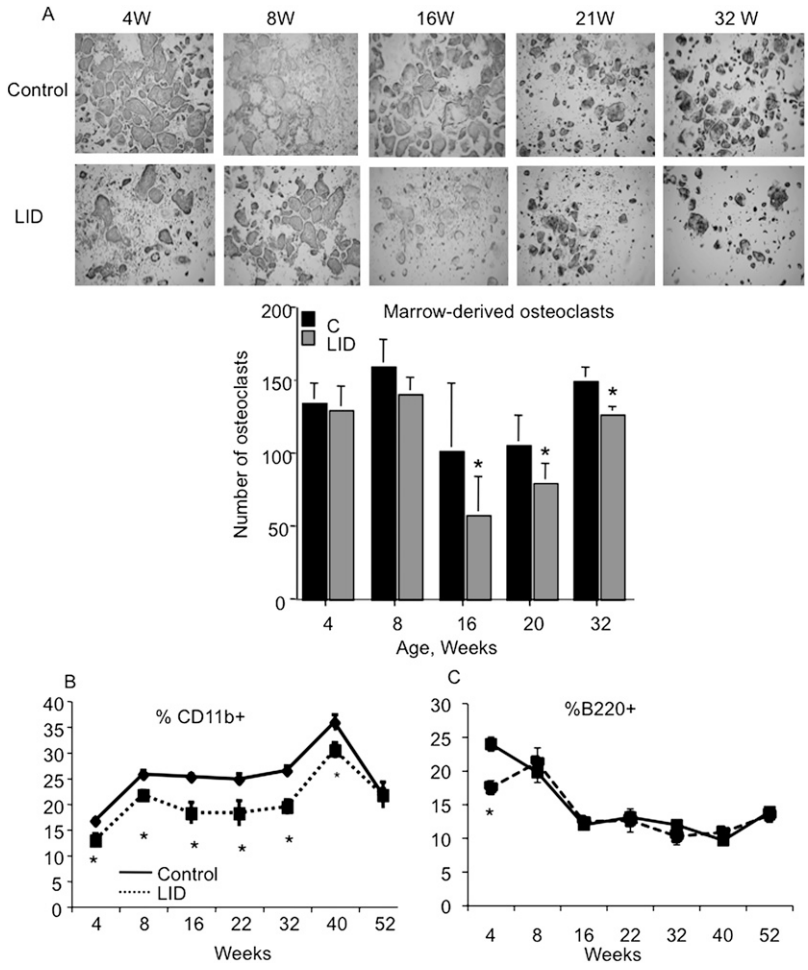

FIG. 5. The number of osteoclast precursors in the nonadherent population derived from LID mice is decreased. Osteoclastogenesis was induced in nonadherent cells derived from marrow of LID and control mice (A). $TRACP^+$ cells were detected after 5–6 days in culture; the bar graph represents quantification of osteoclast number in cultures. FACS analysis of cell surface markers in marrow derived from control and LID mice. Percent of $CD11b^+$ cells was reduced in LID mice throughout development (B), whereas percent $B220^+$ cells reduced significantly only at 4 wk of age. Results are presented as mean ± SE of $n > 8$ mice age per group per genotype.

levels but developed at an early pubertal age affecting mostly transverse bone growth (subperiosteal expansion) and minimally affecting linear growth. These alterations in the proportion of growth in width relative to growth in length lead to the slender adult phenotype of LID mice. This phenotype resulted from different cellular behavior on the endosteal and periosteal surfaces of cortical bone, whereas only minor changes being detected in cancellous bone. A functional analysis showed that morphological compensation for the slender phenotype in LID mice was impaired resulting in limited endosteal apposition (marrow in-filling) and leading to a reduced amount of cortical bone (CtAr) that could be used to construct a mechanically functional bone during growth. Compensatory changes in bone mineralization, which are highly correlated with tissue stiffness,[39] were not evident in LID mice, likely because these variations occur before 4 wk of age[40] and do not depend on serum IGF-1 levels (which normally peak at 3–4 wk) but on skeletal *igf-1* gene expression.

A slender phenotype does not necessarily translate to reduced strength, because bone possesses strong adaptive processes that compensate for the reduced subperiosteal expansion during postnatal growth, a process called ''functional adaptation.'' Thus, finding reduced strength in LID femora, independent of body weight, meant that additional structural or compositional traits, besides impaired subperiosteal expansion, were altered by reduced serum IGF-1. A comparison of femora from C3H/HeJ (high serum IGF-1, small bone diameter), C57BL/6J (low serum IGF-1, large bone diameter), and A/J (low serum IGF-1, small bone diameter; unpublished data) indicated that serum IGF-1 levels are not simply related to bone slenderness. Furthermore, examination of inbred mouse strains with naturally occurring genetic variants leading to slender phenotypes showed that mechanical function was established early postnatally, at ~2 wk of age, through increases in both the relative amount of cortical bone and matrix mineralization.[30,40,41] Surprisingly, reduced levels of serum IGF-1 in LID mice contributed to a slender phenotype only after 4 wk of age, suggesting that additional liver IGF-1–dependent factors expressed early postnatally contributed to the slender adult phenotype. Alternatively, compensatory increases in serum GH before 4 wk in LID mice may account for a normal skeletal phenotype up to 4 wk of age, whereas later in development these increases are not sufficient to establish normal bone function. Furthermore, given the temporal differences in expression of the slender phenotype (between 4 and 8 wk of age) versus

marrow infilling (after 12 wk), we suspect that the impairment of subperiosteal expansion was a direct effect of the reduced serum IGF-1 and that the compensatory response, although impaired, was an indirect effect mediated by the strong adaptive nature of bone.

Although the physiological forces applied to the mouse femur are not known, they are assumed to be proportional to body weight.[4,42,43] Analyses of recombinant inbred mouse strains showed that the Ct.Ar/body weight (BW) relationship (a measure of the amount of bone relative to body weight) is a highly heritable trait.[40] Given the slender phenotype of male LID mice, we expected a tendency toward improved mechanical functionality, namely an increase in Ct.Ar through endosteal apposition. When regressing Tt.Ar/Le against body weight, we found positive relations in control mice such that Tt.Ar/Le increased with body weight. These relationships did not exist in LID mice, indicating that subperiosteal bone expansion was inhibited and requiring that the functional adaptation of LID femora to physiological loads must come through a different mechanism. Whereas control animals did not show any relationship between Ct.Ar/Tt.Ar and body weight, LID mice exhibited a strong, positive relationship between those parameters, suggesting that LID femora adapted to physiological loads through endosteal apposition (i.e., marrow in-filling). Therefore, male LID mice attempted to compensate for the impaired subperiosteal expansion by reversing the net cellular activity from marrow expansion (resorption) to marrow infilling (apposition). This process is similar to the way long bones from female mice adapt to increased body weight during puberty.[41] We expected that the LID mice would show reduced Ct.Ar relative to body weight compared with the controls. This hypothesis was supported, as the LID mice showed a significantly reduced Ct.Ar-BW regression through 52 wk of age. This functional analysis indicated that reduced serum IGF-1 also impaired the amount of tissue that could be used to build a mechanically functional structure. Additionally, despite the shift in functional adaptation from subperiosteal expansion to endosteal bone apposition, the stiffness and strength of LID femora were significantly decreased relative to controls. This was expected, because adding bone to the endosteal surface has limited mechanical benefit to overall bone stiffness and strength. These results indicated that the compensatory increase in endosteal infilling was not fully effective at establishing and maintaining strength for LID femora.

Bone stiffness depends largely on the degree of matrix mineralization.[39] We expected that matrix mineralization would be increased in LID femora to compensate for the slender phenotype. However, matrix mineralization did not differ between LID and controls through 52 wk of age, even when variation in slenderness was corrected for body weight. Ongoing research in our laboratories using inbred mouse models indicated that the functional interactions between bone slenderness and matrix mineralization may begin early postnatally.[40] The degree of mineralization was inversely related to the rate of subperiosteal expansion from 1 day to 4 wk of age. Because endosteal apposition contributes little to overall bone stiffness,[44] the degree of mineralization was a critical factor contributing to the establishment of mechanical function across mice with widely varying growth patterns. The impairment of subperiosteal expansion after 4 wk of age and the lack of a compensatory increase in matrix mineralization for LID femora suggested that the timing in which the reduced serum IGF-1 altered subperiosteal expansion in LID femora may have been a critical factor impairing a compensatory increase in mineralization. Decreased serum IGF-1 levels in LID mice may ultimately have impaired the compensatory changes in mineralization that have been documented in numerous other mouse and human models.[30,39,45] Together with data on inbred mouse strains, it is suggested that, in states of decreased serum IGF-1, achievement of full compensatory interactions (increased Ct.Ar. and TMD) depends on the age at which the genetic variation occurred. In LID mice, reduced serum IGF-1, which normally peaks at 3–4 wk of age, impaired functional adaptation later in growth and thus deleteriously affected skeletal strength by limiting the amount of morphological and compositional compensation.

Impaired functional adaptation results from alterations in bone cell activity. Reduced levels of serum IGF-1 modulate hematopoiesis and can indirectly affect skeletal integrity.[46] In our previous studies, we found a decrease in splenic size in the LID mice, which was attributed to the low levels of serum IGF-1.[29] In this study, we characterized marrow from LID mice and identified a decrease in the $CD11b^+$ cell population throughout growth and aging and a temporal reduction of $B220^+$ cells at early pubertal age. These changes suggested that LID mice exhibit reductions in progenitor cell populations that indirectly may be involved in bone formation and resorption processes.

In summary, our study used established methods for assessing functional adaptation to better evaluate the skeletal phenotype of mice with an engineered mutation that lowered serum IGF-1. This functional analysis, which assessed the co-variation of specific morphological and compositional traits in the context of function, provided a biomechanical mechanism explaining how reduced serum IGF-1 altered bone strength. We showed that serum IGF-1 has two major effects on skeletal integrity: it determines subperiosteal expansion (lateral growth of long bones) and controls the total amount of mineralized cortical tissue that can be deposited during growth (Fig. 6). These two actions of serum IGF-1 require modulation of two cell populations, osteoblasts and osteoclasts, on two spatially distinct bone surfaces (periosteum and endosteum). These surface processes are superimposed on the formation and resorption processes that generate normal cortical drift and permit bone growth to match the overall growth of the animal.[47–49] Consequently, the effects of reduced serum IGF-1 in this study cannot be easily related to traditional measures of osteoblastic and osteoclastic activity. Serum IGF-1 therefore seems to be a master regulator not just of bone size, shape, and composition during growth, but our data suggested that circulating IGF-1 also plays a more fundamental role in skeletal biology—that of regulating an individual's ability to adapt its bone structure to mechanical loads during growth and development.

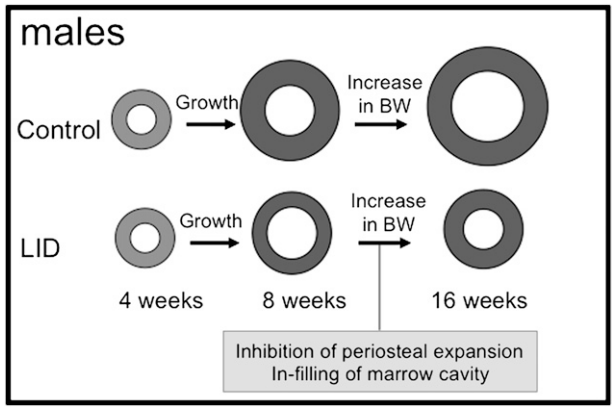

FIG. 6. Schematic representation of the cortical bone envelope during growth. Control mice show a marked increase in cross-sectional area during the first 8 wk of life and later on a slight increase in cross-sectional area associated with expansion of marrow area to allow an efficient structure to support the age-related increase in body weight. LID mice, however, show a marked increase in cross-sectional area during the first 8 wk of life but have a thinner cortical envelope. Later in life, LID mice fail to increase cross-sectional area (because of impaired subperiosteal expansion) and instead show endosteal apposition in an effort to support the age-related increase in body weight.

ACKNOWLEDGMENTS

Financial support was received from funding agencies in the United States: NIH Grants AR054919 (S.Y.), AR055141 (S.Y.), AR44927 (K.J.), and DK42424 (E.C.). The statements made and views expressed are solely the responsibility of the authors.

REFERENCES

1. Langlois JA, Rosen CJ, Visser M, Hannan MT, Harris T, Wilson PW, Kiel DP 1998 Association between insulin-like growth factor I and bone mineral density in older women and men: The Framingham Heart Study. J Clin Endocrinol Metab **83:**4257–4262.
2. Garnero P, Sornay-Rendu E, Delmas PD 2000 Low serum IGF-1 and occurrence of osteoporotic fractures in postmenopausal women. Lancet **355:**898–899.
3. Turner CH 1992 Functional determinants of bone structure: Beyond Wolff's law of bone transformation. Bone **13:**403–409.
4. Beck TJ, Ruff CB, Mourtada FA, Shaffer RA, Maxwell-Williams K, Kao GL, Sartoris DJ, Brodine S 1996 Dual-energy X-ray absorptiometry derived structural geometry for stress fracture prediction in male U.S. Marine Corps recruits. J Bone Miner Res **11:**645–653.
5. Black DM, Bouxsein ML, Marshall LM, Cummings SR, Lang TF, Cauley JA, Ensrud KE, Nielson CM, Orwoll ES 2008 Proximal femoral structure and the prediction of hip fracture in men: A large prospective study using QCT. J Bone Miner Res **23:**1326–1333.
6. Rivadeneira F, Zillikens MC, De Laet CE, Hofman A, Uitterlinden AG, Beck TJ, Pols HA 2007 Femoral neck BMD is a strong predictor of hip fracture susceptibility in elderly men and women because it detects cortical bone instability: The Rotterdam Study. J Bone Miner Res **22:**1781–1790.
7. Zebaze RM, Jones A, Knackstedt M, Maalouf G, Seeman E 2007 Construction of the femoral neck during growth determines its strength in old age. J Bone Miner Res **22:**1055–1061.
8. Beamer WG, Donahue LR, Rosen CJ, Baylink DJ 1996 Genetic variability in adult bone density among inbred strains of mice. Bone **18:**397–403.
9. Koller DL, Schriefer J, Sun Q, Shultz KL, Donahue LR, Rosen CJ, Foroud T, Beamer WG, Turner CH 2003 Genetic effects for femoral biomechanics, structure, and density in C57BL/6J and C3H/HeJ inbred mouse strains. J Bone Miner Res **18:**1758–1765.
10. Rosen CJ, Dimai HP, Vereault D, Donahue LR, Beamer WG, Farley J, Linkhart S, Linkhart T, Mohan S, Baylink DJ 1997 Circulating and skeletal insulin-like growth factor-I (IGF-I) concentrations in two inbred strains of mice with different bone mineral densities. Bone **21:**217–223.
11. Alam I, Sun Q, Liu L, Koller DL, Fishburn T, Carr LG, Econs MJ, Foroud T, Turner CH 2005 Whole-genome scan for linkage to bone strength and structure in inbred Fischer 344 and Lewis rats. J Bone Miner Res **20:**1589–1596.
12. Bouxsein ML, Uchiyama T, Rosen CJ, Shultz KL, Donahue LR, Turner CH, Sen S, Churchill GA, Muller R, Beamer WG 2004 Mapping quantitative trait loci for vertebral trabecular bone volume fraction and microarchitecture in mice. J Bone Miner Res **19:**587–599.
13. Klein RF, Turner RJ, Skinner LD, Vartanian KA, Serang M, Carlos AS, Shea M, Belknap JK, Orwoll ES 2002 Mapping quantitative trait loci that influence femoral cross-sectional area in mice. J Bone Miner Res **17:**1752–1760.
14. Rosen CJ, Beamer WG, Donahue LR 2001 Defining the genetics of osteoporosis: Using the mouse to understand man. Osteoporos Int **12:**803–810.
15. Rosen CJ, Churchill GA, Donahue LR, Shultz KL, Burgess JK, Powell DR, Ackert C, Beamer WG 2000 Mapping quantitative trait loci for serum insulin-like growth factor-1 levels in mice. Bone **27:**521–528.
16. Mora S, Pitukcheewanont P, Nelson JC, Gilsanz V 1999 Serum levels of insulin-like growth factor I and the density, volume, and cross-sectional area of cortical bone in children. J Clin Endocrinol Metab **84:**2780–2783.
17. Gross TS, Srinivasan S, Liu CC, Clemens TL, Bain SD 2002 Noninvasive loading of the murine tibia: An in vivo model for the study of mechanotransduction. J Bone Miner Res **17:**493–501.
18. Slootweg MC, Hoogerbrugge CM, de Poorter TL, Duursma SA, van Buul-Offers SC 1990 The presence of classical insulin-like growth factor (IGF) type-I and -II receptors on mouse osteoblasts: Autocrine/paracrine growth effect of IGFs? J Endocrinol **125:**271–277.
19. Mochizuki H, Hakeda Y, Wakatsuki N, Usui N, Akashi S, Sato T, Tanaka K, Kumegawa M 1992 Insulin-like growth factor-I supports formation and activation of osteoclasts. Endocrinology **131:**1075–1080.
20. Rubin J, Ackert-Bicknell CL, Zhu L, Fan X, Murphy TC, Nanes MS, Marcus R, Holloway L, Beamer WG, Rosen CJ 2002 IGF-I regulates osteoprotegerin (OPG) and receptor activator of nuclear factor-kappaB ligand in vitro and OPG in vivo. J Clin Endocrinol Metab **87:**4273–4279.
21. Zhang M, Xuan S, Bouxsein ML, von Stechow D, Akeno N, Faugere MC, Malluche H, Zhao G, Rosen CJ, Efstratiadis A, Clemens TL 2002 Osteoblast-specific knockout of the insulin-like growth factor (IGF) receptor gene reveals an essential role of IGF signaling in bone matrix mineralization. J Biol Chem **277:**44005–44012.
22. Jiang J, Lichtler AC, Gronowicz GA, Adams DJ, Clark SH, Rosen CJ, Kream BE 2006 Transgenic mice with osteoblast-targeted insulin-like growth factor-I show increased bone remodeling. Bone **39:**494–504.
23. Mohan S, Baylink DJ 2005 Impaired skeletal growth in mice with haploinsufficiency of IGF-I: Genetic evidence that differences in IGF-I expression could contribute to peak bone mineral density differences. J Endocrinol **185:**415–420.
24. Mathews LS, Hammer RE, Behringer RR, D'Ercole AJ, Bell GI, Brinster RL, Palmiter RD 1988 Growth enhancement of transgenic mice expressing human insulin-like growth factor I. Endocrinology **123:**2827–2833.

25. Efstratiadis A 1998 Genetics of mouse growth. Int J Dev Biol **42:**955–976.
26. Liu JP, Baker J, Perkins AS, Robertson EJ, Efstratiadis A 1993 Mice carrying null mutations of the genes encoding insulin-like growth factor I (Igf-1) and type 1 IGF receptor (Igf1r). Cell **75:**59–72.
27. Yakar S, Liu JL, Stannard B, Butler A, Accili D, Sauer B, LeRoith D 1999 Normal growth and development in the absence of hepatic insulin-like growth factor I. Proc Natl Acad Sci USA **96:**7324–7329.
28. Yakar S, Bouxsein ML, Canalis E, Sun H, Glatt V, Gundberg C, Cohen P, Hwang D, Boisclair Y, Leroith D, Rosen CJ 2006 The ternary IGF complex influences postnatal bone acquisition and the skeletal response to intermittent parathyroid hormone. J Endocrinol **189:**289–299.
29. Yakar S, Rosen CJ, Beamer WG, Ackert-Bicknell CL, Wu Y, Liu JL, Ooi GT, Setser J, Frystyk J, Boisclair YR, LeRoith D 2002 Circulating levels of IGF-1 directly regulate bone growth and density. J Clin Invest **110:**771–781.
30. Jepsen KJ, Hu B, Tommasini SM, Courtland HW, Price C, Terranova CJ, Nadeau JH 2007 Genetic randomization reveals functional relationships among morphologic and tissue-quality traits that contribute to bone strength and fragility. Mamm Genome **18:**492–507.
31. Yakar S, Setser J, Zhao H, Stannard B, Haluzik M, Glatt V, Bouxsein ML, Kopchick JJ, LeRoith D 2004 Inhibition of growth hormone action improves insulin sensitivity in liver IGF-1-deficient mice. J Clin Invest **113:**96–105.
32. Silha JV, Gui Y, Mishra S, Leckstrom A, Cohen P, Murphy LJ 2005 Overexpression of gly56/gly80/gly81-mutant insulin-like growth factor-binding protein-3 in transgenic mice. Endocrinology **146:**1523–1531.
33. Laib A, Hildebrand T, Hauselmann HJ, Ruegsegger P 1997 Ridge number density: A new parameter for in vivo bone structure analysis. Bone **21:**541–546.
34. Hildebrand T, Ruegsegger P 1997 A new method for the model independent assessment of thickness in three-dimensional images. J Microsc **185:**67–75.
35. Otsu N 1979 A threshold selection method from gray-level histograms. IEEE Trans Syst Man Cybern **9:**62–66.
36. Parfitt AM, Drezner MK, Glorieux FH, Kanis JA, Malluche H, Meunier PJ, Ott SM, Recker RR 1987 Bone histomorphometry: Standardization of nomenclature, symbols, and units. Report of the ASBMR Histomorphometry Nomenclature Committee. J Bone Miner Res **2:**595–610.
37. Scharf J, Ramadori G, Braulke T, Hartmann H 1996 Synthesis of insulinlike growth factor binding proteins and of the acid-labile subunit in primary cultures of rat hepatocytes, of Kupffer cells, and in cocultures: Regulation by insulin, insulinlike growth factor, and growth hormone. Hepatology **23:**818–827.
38. Ooi GT, Orlowski CC, Brown AL, Becker RE, Unterman TG, Rechler MM 1990 Different tissue distribution and hormonal regulation of messenger RNAs encoding rat insulin-like growth factor-binding proteins-1 and -2. Mol Endocrinol **4:**321–328.
39. Courtland HW, Nasser P, Goldstone AB, Spevak L, Boskey AL, Jepsen KJ 2008 Fourier transform infrared imaging microspectroscopy and tissue-level mechanical testing reveal intraspecies variation in mouse bone mineral and matrix composition. Calcif Tissue Int **83:**342–353.
40. Jepsen KJHB, Tommasini SM, Courtland H-W, Price C, Cordova M, Nadeau JH 2009 Phenotypic integration of skeletal traits during growth buffers genetic variants affecting the slenderness of femora in inbred mouse strains. Mamm Genome **20:**21–33.
41. Price C, Herman BC, Lufkin T, Goldman HM, Jepsen KJ 2005 Genetic variation in bone growth patterns defines adult mouse bone fragility. J Bone Miner Res **20:**1983–1991.
42. Carter DR, Wong M, Orr TE 1991 Musculoskeletal ontogeny, phylogeny, and functional adaptation. J Biomech **24**(Suppl 1)**:**3–16.
43. Moro M, van der Meulen MC, Kiratli BJ, Marcus R, Bachrach LK, Carter DR 1996 Body mass is the primary determinant of midfemoral bone acquisition during adolescent growth. Bone **19:**519–526.
44. van der Meulen MC, Jepsen KJ, Mikic B 2001 Understanding bone strength: Size isn't everything. Bone **29:**101–104.
45. Tommasini SM, Nasser P, Schaffler MB, Jepsen KJ 2005 Relationship between bone morphology and bone quality in male tibias: Implications for stress fracture risk. J Bone Miner Res **20:**1372–1380.
46. Lorenzo J, Horowitz M, Choi Y 2008 Osteoimmunology: Interactions of the bone and immune system. Endocr Rev **29:**403–440.
47. Epker BN, Frost HM 1965 The direction of transverse drift of actively forming osteons in human rib cortex. J Bone Joint Surg Am **47:**1211–1215.
48. Epker BN, Frost HM 1966 Biomechanical control of bone growth and development: A histologic and tetracycline study. J Dent Res **45:**364–371.
49. Epker BN, Frost HM 1966 Periosteal appositional bone growth from age two to age seventy in man. A tetracycline evaluation. Anat Rec **154:**573–577.

Received in original form November 28, 2008; revised form December 31, 2008; accepted February 12, 2009.